UNIVERSIDADE DO VALE DO RIO DOS SINOS - UNISINOS
UNIDADE ACADÊMICA DE PESQUISA E PÓS-GRADUAÇÃO

PROGRAMA DE PÓS-GRADUAÇÃO em GEOLOGIA

Nome do Autor: Gustavo Nunes Aumond

Título: CONSIDERAÇÕES PALEOAMBIENTAIS E PALEOCLIMÁTICAS SOBRE O "MAR ENTRERRIENSE" DO MIOCENO TARDIO: ESTUDO DE CASO DA FORMAÇÃO CAMACHO, URUGUAI

Nível: Mestrado

Data de Defesa: 01/03/2021

E-mail de Contato do Autor: gustavo.aumond@gmail.com

UNIVERSIDADE DO VALE DO RIO DOS SINOS - UNISINOS
UNIDADE ACADÊMICA DE PESQUISA E PÓS-GRADUAÇÃO
PROGRAMA DE PÓS-GRADUAÇÃO EM GEOLOGIA
NÍVEL MESTRADO

DEFESA DE MESTRADO

CONSIDERAÇÕES PALEOAMBIENTAIS E PALEOCLIMÁTICAS SOBRE O "MAR ENTRERRIENSE" DO MIOCENO TARDIO: ESTUDO DE CASO DA FORMAÇÃO CAMACHO, URUGUAI

GUSTAVO NUNES AUMOND

São Leopoldo
2021

Gustavo Nunes Aumond

CONSIDERAÇÕES PALEOAMBIENTAIS E PALEOCLIMÁTICAS SOBRE O "MAR ENTRERRIENSE" DO MIOCENO TARDIO: ESTUDO DE CASO DA FORMAÇÃO CAMACHO, URUGUAI

Área de Concentração: Geologia Sedimentar
Linha de Pesquisa: Paleontologia Aplicada
Tema de interesse: Geoquímica – Estratigrafia

Este documento aborda a contextualização teórica, bem como o arcabouço científico que embasa a discussão da dissertação de mestrado, assim como seus resultados.

Orientador: Prof. Dr. Karlos G. D. Kochhann

A925c Aumond, Gustavo Nunes.

Considerações paleoambientais e paleoclimáticas sobre o “Mar Entrerriense” do mioceno tardio : estudo de caso da Formação Camacho, Uruguai / Gustavo Nunes Aumond. – 2021.

45 f. : il. ; 30 cm.

Dissertação (mestrado) – Universidade do Vale do Rio dos Sinos, Programa de Pós-Graduação em Geologia, 2021.

“Orientador: Prof. Dr. Karlos G. D. Kochhann.”

Dados Internacionais de Catalogação na Publicação (CIP)

(Bibliotecária: Amanda Schuster – CRB 10/2517)

SUMÁRIO

RESUMO

Durante o Mioceno, ocorreram diversas incursões marinhas sobre o continente Sul-Americano. Oscilações no clima provocaram retração ou expansão da cobertura de gelo das áreas polares, causando variações do nível do mar registradas em áreas costeiras como eventos transgressivos/regressivos. Na costa sudeste do Uruguai, no Departamento de Colonia, afloram depósitos de uma destas ingressões marinhas, denominada "Mar Entrerriense", e seus depósitos caracterizam a Formação Camacho, de idade Mioceno tardio. Buscando melhor entender as condições paleoambientais e a configuração paleoclimática registradas pelos estratos da Formação Camacho, o presente estudo apresenta uma análise de alta resolução multi-*proxy*, aplicando análises de FRX (florescência de Raios-X), COT (carbono Orgânico Total), TS (Enxofre Total), conteúdo de carbonatos, refletância espectral e análises de fácies e icnológicas, dos depósitos aflorantes no sudoeste do Uruguai. Os resultados sugerem deposição em ambientes marinhos rasos, com águas bem oxigenadas, e sob a influência de processos de energia moderada a baixa, com deposição afetada por correntes de maré e eventos de tempestade. Os registros das razão hematita/goetita, log(Zr/Rb), log(Ti/Rb) e Sr/Ba, sugerem uma tendência de raseamento para o topo da seção marinha da Formação Camacho na área de estudo, acompanhada de tendência de maior proximidade em relação à área fonte, do estabelecimento de paleoclimas mais úmidos e da maior influência de aporte de água doce em direção ao topo da seção, o que é corroborado pelas mudanças no padrão das icnofábricas. Os padrões sedimentares e geoquímicos descritos nesse estudo para a Formação Camacho estão provavelmente relacionados ao resfriamento de altas latitudes e à consequente queda do nível do mar iniciados há ~7.2 Ma.

APRESENTAÇÃO

O Mioceno, intervalo de tempo entre 23,03 e 5,33 Ma (Ogg et al., 2016), é marcado por variações climáticas abruptas, como o evento de aquecimento global entre 16,9 e 14,7 Ma, conhecido como Ótimo Climático do Mioceno (OCM)), e os eventos de resfriamentos há ~14, ~10 e ~7 Ma (e.g. Holbourn et al., 2018; Kochhann et al., 2017). Essas variações climáticas causaram expansão e retração de gelo nas áreas polares (e.g. Zachos et al., 2001), associadas a variações do nível do mar, tendo como consequência o registro de eventos transgressivos/regressivos em sucessões sedimentares marginais marinhas (Miller et al., 2017).

A sedimentação miocênica no continente Sul-Americano é caracterizada por diversos depósitos relacionados a eventos transgressivos, durante os quais as águas do Oceano Atlântico avançaram sobre regiões até então continentais, deixando registros sedimentares na Argentina, Paraguai, Brasil e nos departamentos de Colônia e San José, na República do Uruguai. Este avanço marinho sobre a costa é conhecido como “Mar Entrerriense” e seus depósitos no Uruguai são atribuídos à Formação Camacho. A formação é subdividida litologicamente em Membro San Pedro, na base da formação, e Membro Cerro Bautista, no topo (Perea e Martínez, 2004). Os depósitos relacionados à Formação Camacho são ricos em fósseis marinhos, sendo considerada uma das mais ricas faunas fósseis do país, e apresentam também um conjunto importante de mamíferos continentais, icnofóssies e microfósseis (Perea et al., 2011). Análises de isótopos de estrôncio (Sr) em fósseis de moluscos marinhos e a bioestratigrafia dos fósseis indicam uma idade miocênica tardia para a Formação Camacho (del Río et al., 2018).

Proxies geoquímicos em sedimentos e rochas sedimentares têm sido usados globalmente para interpretações paleoambientais e paleoclimáticas nesse intervalo de tempo (e.g. Wei et al., 2006; Köhler et al., 2010; Yang et al., 2019). Informações como padrões de

intemperismo atuantes, condições de deposição, salinidade e oxigenação de massa de água, condições climáticas, entre outras variáveis, podem ser estimadas utilizando-se essas ferramentas. Contudo, os estratos da Formação Camacho ainda não foram analisados por técnicas geoquímicas em alta resolução temporal. O presente trabalho visa preencher essa lacuna, reconstituindo as condições paleoambientais vigentes durante a deposição dos estratos marinhos da Formação Camacho, com base em dados geoquímicos e propriedades físicas e biogênicas dos sedimentos. Pretende-se, ainda, relacionar os padrões reconhecidos na Formação Camacho com variações paleoclimáticas regionais e/ou globais registradas durante o Mioceno. A hipótese a ser testada neste estudo é de que a Formação Camacho registra as condições paleoambientais de um evento transgressivo-regressivo associado a variações climáticas globais ocorridas durante o Mioceno.

Os resultados obtidos neste estudo foram submetidos ao periódico *Journal of South American Earth Sciences*, conceito Qualis-CAPES B1.

COMPROVANTE DE SUBMISSÃO

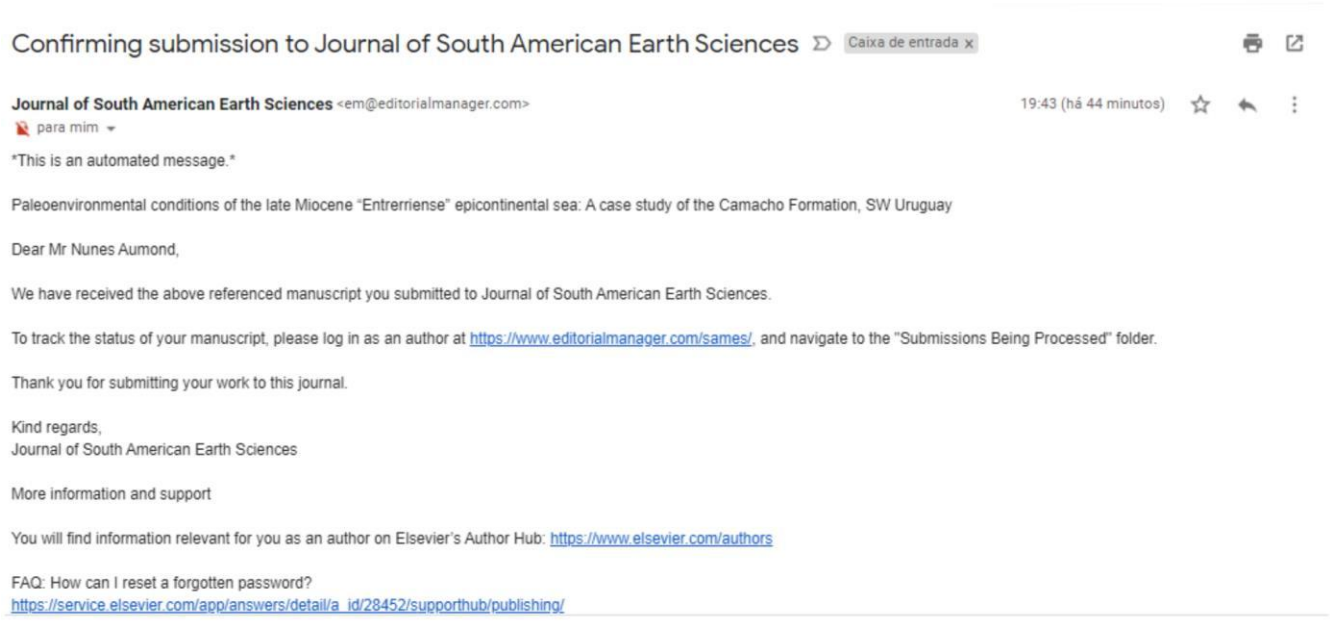

Confirming submission to Journal of South American Earth Sciences Caixa de entrada x

Journal of South American Earth Sciences <em@editorialmanager.com> 19:43 (há 44 minutos)

para mim

This is an automated message.

Paleoenvironmental conditions of the late Miocene "Entrerriense" epicontinental sea: A case study of the Camacho Formation, SW Uruguay

Dear Mr Nunes Aumond,

We have received the above referenced manuscript you submitted to Journal of South American Earth Sciences.

To track the status of your manuscript, please log in as an author at https://www.editorialmanager.com/sames/, and navigate to the "Submissions Being Processed" folder.

Thank you for submitting your work to this journal.

Kind regards,
Journal of South American Earth Sciences

More information and support

You will find information relevant for you as an author on Elsevier's Author Hub: https://www.elsevier.com/authors

FAQ: How can I reset a forgotten password?
https://service.elsevier.com/app/answers/detail/a_id/28452/supporthub/publishing/

Paleoenvironmental conditions of the late Miocene "Entrerriense" epicontinental sea: A case study of the Camacho Formation, SW Uruguay

Gustavo N. Aumond[a], Karlos G. D. Kochhann[a], Renata G. Netto[a], Laís V. de Souza[b], Daniel Sedorko[c], Rodrigo S. Horodyski[a] ,Flavio N. Almeida Júnior[d].

[a] Geology Graduate Program, Unisinos University – Av. Unisinos, 950 – Bairro Cristo Rei, São Leopoldo/RS – Brazil. gustavo.aumond@gmail.com, kkochhann@unisinos.br, nettorg@unisinos.br

[b] VizGEO Lab, Unisinos University – Av. Unisinos, 950 – Bairro Cristo Rei, São Leopoldo/RS – Brazil. laisvs@unisinos.br

[c] Labortório de Paleontologia Estratigráfica, Geography Institute, Federal University of Uberlândia. Av. XV de novembro, 501, Boa Vista. Monte Carmelo – MG, 38500-000, Brazil. sedorko@ufu.br

[d] Department of Earth Science, University of Bergen, Allégaten 41, 5007, Bergen, Norway. Flavio.DeAlmeida@uib.no

Corresponding author: *Gustavo N. Aumond, gustavo.aumond@gmail.com*

HIGHLIGHTS

- The Camacho Formation records a shallowing-upward trend in a shallow marine setting
- Gradually more proximal settings were likely related to sea level fall at 7.2-6.5 Ma
- Paleoclimate became progressively wetter within the studied succession
- Uppermost strata of the Camacho Formation record increased freshwater influence

ABSTRACT

Marine sediments deposited during late Miocene transgressive events are recorded over large onshore areas in southeastern South America, characterizing the "Entrerriense Sea". In Uruguay, these deposits outcrop at the coast of the Department of Colonia, and are assigned to

the Camacho Formation, which is well-known by its abundant fossil content. Nevertheless, studies applying geochemical proxies in the Camacho Formation are not yet available. Our goals are: (1) to assess in high resolution paleoenvironmental changes recorded by the marine and/or marine-influenced strata of the Camacho Formation in Uruguay; (2) to explore possible links between local responses and global climate shifts that occurred during the late Miocene. To achieve these goals, we applied a multi-proxy approach, in which sedimentary facies and trace fossil occurrences were compared with geochemical and physical properties records measured in high-resolution along the exposed sedimentary succession of the Camacho Formation. Our results suggest that these strata record a shallowing-upward trend, also characterized by deposition in gradually more proximal settings [increasing-upward trends in log(Zr/Rb) and log(Ti/Rb)], coupled to increased influence of freshwater input in the upper half of the studied sedimentary succession (decreasing-upward Sr/Ba trend). Considering previously published ages for the Camacho Formation, we infer that this shallowing-upward trend was related to the high latitude cooling and/or ice volume expansion occurred between 7.2 and 6.9 Ma, and the associated long-term sea level fall from 7.2 to 6.5 Ma. These trends occurred in tandem with the onset of more humid climate conditions (recorded on the uppermost strata of the Camacho Formation), which were likely related to the latitudinal migration of climatic belts.

Keywords: Paleoenviromental proxies, Tortonian-Messinian, fossil-rich strata, “Paranense Sea”, climate change.

1. Introduction

In South America, marine sediments deposited during late Miocene transgressive events are recorded in Argentina, Paraguay, Brazil, and Uruguay (e.g., Perea, 2004; Perea et al., 2011; del Río et al., 2018). These strata are commonly interpreted as the record of an

epicontinetal sea known as “Entrerriense Sea” (or “Paranense Sea”), which in Uruguay is represented by the fossil-rich Camacho Formation (Perea et al., 2011). The fossil content of the Camacho Formation includes marine invertebrates, mammals, microfossils, and trace fossils (e.g., Mones, 1979; Perea and Ubilla, 1990; Martinez, 1994; del Río, 1998; Soibelzon et al., 2019; Perea et al., 2020). These fossil assemblages were first assigned to the Pliocene (Kraglievich, 1928; Teisseire, 1928; Walther, 1931; Lambert, 1940; Serra, l943; Caorsi and Goñi, 1958; Goñi and Hoffstetter, l964; Goso and Bossi, 1966; Francis, l975; Sprechmann, 1978; Martinez, 1994), however more recent studies agree in a Tortonian-Messinian (late Miocene) age for the deposition of the Camacho Formation (see Section 2). The Camacho Formation is temporally correlated with the Paraná Formação (Chaco-Paranense Basin), “Entrerrienses beds” (Salado Basin), as well as the Barranca Final Formation and Facies Balneario La Lobería (Colorado Basin) in Argentina (Wahnish, 1939; Serra, 1943; Goso and Bossi, 1966; Aceñolaza, 1976, 2000; Haller, 1978; Angulo and Casamiquela, 1982; Scasso and del Río, 1987; Marengo, 2015; Del Río et al., 2018).

Since Charles Darwin first mentioned fossil-rich strata in the Department of Colonia (Uruguay) in 1839, several studies focusing on the taxonomy, biostratigraphy, and paleoenvironmental significance of the fossil assemblages of the Camacho Formation were carried out (e.g., Closs and Madeira, 1968; Figueiras and Broggi, l97l; Sprechmann 1978, 1980; Herbste and Zabert, 1979, 1987; Marshall et al., 1983; 1989; Martinez, 1994). These paleontological studies mostly suggest deposition in an inner shelf setting with normal marine, or slightly reduced salinity (Martínez, 1994; Perea and Martínez, 2004). Paralic conditions were also inferred from vertebrate assemblages of the Camacho Formation (Perea and Martínez, 2004). One limitation of these paleoenvironmental reconstructions based on fossils is that they usually provide an overall characterization for the Camacho Formation, making it difficult to access gradual trends within the sedimentary succession.

Studies based on geochemical proxies have been used around the world to assist in high-resolution paleoenvironmental and paleoclimatic interpretations for the Miocene (e.g., Wei et al., 2006; Köhler et. al. 2010; Yang et al., 2019). Analysis of geochemical proxies can help, for example, to reconstruct weathering and climate patterns, depositional settings, among other parameters (e.g., Weaver, 1967, 1989; Niebuhr, 2005). However, proxy records measured in high-resolution along the Camacho Formation are not yet available, hampering high-resolution paleoenvironmental reconstructions.

Here we applied a multi-proxy approach by comparing sedimentary facies and trace fossil content with geochemical and physical properties of the sediments measured in high-resolution along the sedimentary succession of the Camacho Formation cropping out at the margin of the La Plata Estuary, southwestern Uruguay. Our objectives are (1) to assess in high-resolution paleoenvironmental changes recorded in the marine and/or marine-influenced strata from the Camacho Formation, and (2) to explore possible links between local responses and global climate changes occurred during the late Miocene.

2. Geological setting and study area

The Camacho Formation crops out in the departaments of Colonia and San José, and also occurs at subsurface in the San José, Maldonado, and Rocha departments (Perea and Martínez, 2004). In the studied area, the Camacho Formation is lithologically subdivided into two members, the San Pedro Member at the base, composed of silty to sandy deposits, and the Cerro Bautista Member at the top, characterized by very fine to fine-grained sandstone interbedded with coarser deposits (Perea and Martínez, 2004). Deposition in a marine setting is evidenced by fossil occurrences of mollusks (gastropods and bivalves), echinoderms, crustaceans, brachiopods, bryozoans, sharks, bony fishes, whales, and dolphins (Perea et al., 2011). At certain stratigraphic levels, these fossil remains occur as shell beds, like proximal

tempestites (e.g., Simões and Torello, 2003), suggesting deposition at shallow paleodepths (Matínez and Perea, 2004).

Overall, biostratigraphic evidence points to a Tortonian-Messinian (late Miocene) age for the Camacho Formation (Figueiras and Broglie, 1971; Herbst and Zaberst, 1979, 1987; Perea and Martínez , 2011; Perea et al., 2013, 2020). Likewise, Sr^{87}/Sr^{86} values measured in mollusks (Pectinidae) suggest numerical ages between 7.2 and 6.0 Ma, within the Messinian, for the Camacho Formation (del Río et al., 2018). Somewhat different age assignments of ~17-15 Ma (middle Miocene), based on Sr^{87}/Sr^{86} values measured in brackish water oysters, were reported by Sprechmann et al. (2010).

We analyzed samples from two outcrop sections in the Department of Colonia, Uruguay: San Pedro section (FC01; 5 m thick; 34º 20´58.0” S, 57º 55´01.2” W) and El Chileno (FC02; 4.5 m thick; 34º 21´41.0” S, 57º54´30.5” W) (Fig. 1 and 2A, B). These outcrops present a lateral extension of about 800 m at the Uruguayan margin of the La Plata Estuary. Sampling was conducted in high-resolution (10 cm spacing) (Fig. 2C), totaling 47 samples for section FC01 and 30 samples for section FC02.

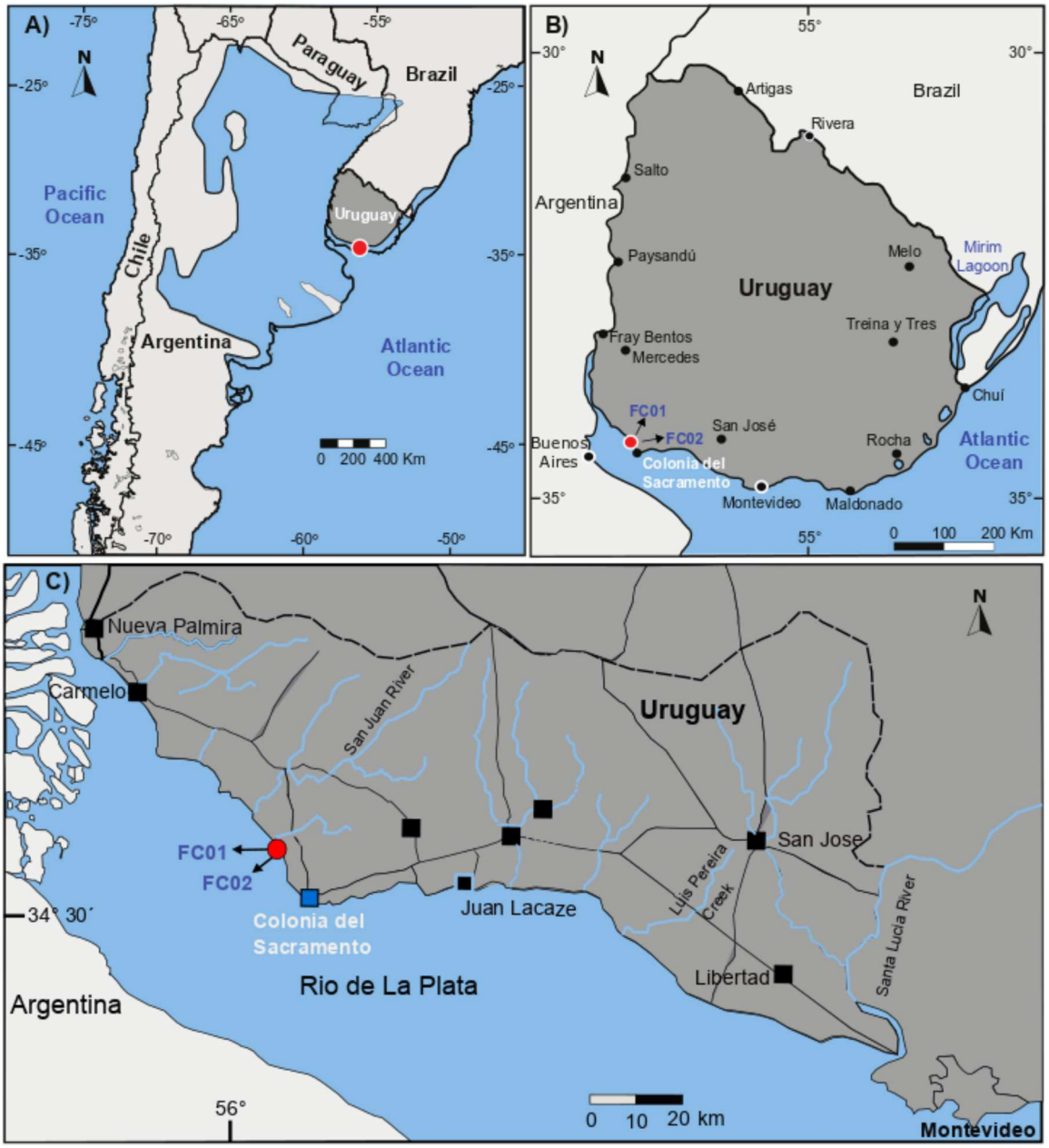

Figure 1. Location map of the studied area. A) Reconstructed extension of the "Entrerriense Sea" transgression over South America. B) Location of the studied outcrops in southwestern Uruguay. C) Detail Location of the studied outcrops in the Department of Colonia, Uruguai. The San Pedro (FC01) and El Chileno (FC02) outcrops are shown as red circles; in C, black lines represent main roads and blue lines represent drainages. Maps modified from Palacio et al. (2016), Perea et al. (2011) and Matinez and Sergio (1994).

Figure 2. Sedimentary facies from Camacho Formation. A – General view of the San Pedro outcrop (FC01); B - General view of the El Chileno outcrop (FC02); C – Detail of regularly spaced collected samples; D – E. Detail of highly-bioturbated sandy siltstone (D) interbedded with an oyster bank (E). F – Cycles of fine-grained heterolithic beds (very fine-grained sandstone, siltstone, and claystone) capped by fine-grained sandstone with wave bedding. G - Fine-grained sandstone beds at top of El Chileno outcrop. H, I – Gently lenticular sandstone beds, forming a quasi-tabular geometry (H) and hummocky cross-stratification (I).

3. Material and methods

3.1. X-ray fluorescence (XRF) analysis

For each sample, about 10 g of dried sediments were ground in an agate mortar, placed in a sample container, covered with a polyester film, and then analyzed in a Panalytical Epsylon 1 XRF spectrometer at the Technological Institute for Paleoceanography and Climate Changes (iit OCEANEON, UNISINOS University). Results were reported as raw elemental intensities (counts per second - cps) and were mostly interpreted in terms of logarithmic elemental ratios. We used different voltages to detect specific groups of elements: 10 kV for Al, Mg and Si; 12 kV for Ca, K, Ti and V; 20 kV for Co, Cr, Fe and Mn; 50 kV for Ba and Rb. Average analysis time was about six minutes per sample.

We used log(Zr/Rb) as a proxy for sediment grain size changes (e.g., Weaver, 1967, 1989; Niebuhr, 2005), log(Ti/Rb) to infer distance from the sediment source area (e.g., Spofforth et al., 2008), log(K/Al) to reconstruct weathering patterns at the source area (e.g., Weaver, 1967, 1989; Niebuhr, 2005), and Sr/Ba to track changes is water salinity (Wei and Algeo, 2020). Detailed discussions about the application of these elemental ratios as paleoenvironmental proxies are provided in Section 5.1. XRF-derived data are available in supplementary table S1.

3.2. Calcium carbonate ($CaCO_3$), total organic carbon (TOC), and total sulfur (TS) contents

To measure TOC, $CaCO_3$, and TS we used a sediment aliquot of ~0.6 g for each dry ground sample. We measured total carbon (TC) and TS on ~0.26 g aliquots by total combustion, after addition of the catalyst vanadium pentoxide, using a LECO SC-144DR at itt OCEANEON. TOC was also measured on ~0.26 g aliquots, after acidification with HCl 6 N (1:1), followed by washing with deionized water (until pH = 5 was reached), and drying at 40 °C. Carbonate content was calculated with the equation $CaCO_3\%$ = [TC(%) – TOC (%)] *

8.33 (Stax and Stein, 1993). TOC, $CaCO_3$, and TS contents are available in supplementary table S1.

3.3. Spectral reflectance

We measured spectral reflectance on 5 g of the ground samples with a portable high-resolution spectroradiometer Spectral Evolution® SR-35000 at VizLab (UNISINOS University). We measured 1024 spectral bands between ultraviolet and shortwave infrared (0.35 to 2.5 μm), with a mean acquisition time of 2 seconds. The spectroradiometer was calibrated using a white reflectance Spectralon® plate before the first scan and after every six measurements. We performed three measurements per sample and worked with the average value for each spectral band in order to minimize analytical variability.

We analyzed the spectral reflectance patterns of our samples by graphically comparing wavelengths versus reflectance values. To identify the minerals responsible for the observed absorption features, we compared our samples with mineral spectra from the United States Geological Survey (USGS) library (Clark et al., 2007), especially with samples CM20 (montmorillonite) and AMX15 (calcite + montmorillonite). The ratio of 565/435 color intensities, also known as the hematite/goethite ratio, was applied as a proxy for weathering conditions. Hematite is predominantly formed under humid conditions, while goethite formation is favored under more arid conditions (e.g., Giosan et al., 2002; Clift, 2006). Spectral reflectance data are available in supplementary table S2.

3.4. Composite section

Since strata gently dip in the studied area, and parts of the studied outcrops overlap, we generated a composite section from FC01 and FC02 based on the correlation of sedimentological, geochemical, and ichnological data. The ichnological data is restricted to

the ichnofabric approach and the ichnogeneric composition of ichnofabrics is based on the ichnotaxonomical characterization made by Verde (2002) and Verde and Martinez (2004). Each individual section log is also presented (online supplementary figures S1 and S2), however, our interpretations are presented only for the composite section (Fig. 3).

Our data suggest that the basal 1.2 m at the FC01 outcrop are laterally equivalent to the 0-3.2 m interval at the FC02 outcrop. These intervals present comparable fine-grained sediments and ichnofabrics, relatively low log(Zr/Rb) and log(Ti/Rb), and relatively high log(K/Al). To accommodate these observations, we correlated the increasing-upward trend in sediment grain size between 2.8 and 3.2 m at FC01 to the increasing trend in log(Zr/Rb), also suggesting increasing grain sizes (e.g., Spofforth et al., 2008; Beil et al., 2018), between 1.0 and 1.4 at FC02. Our correlation tie point between the two outcrops is placed at 1.4 m in FC01 and at 3.2 m in FC02.

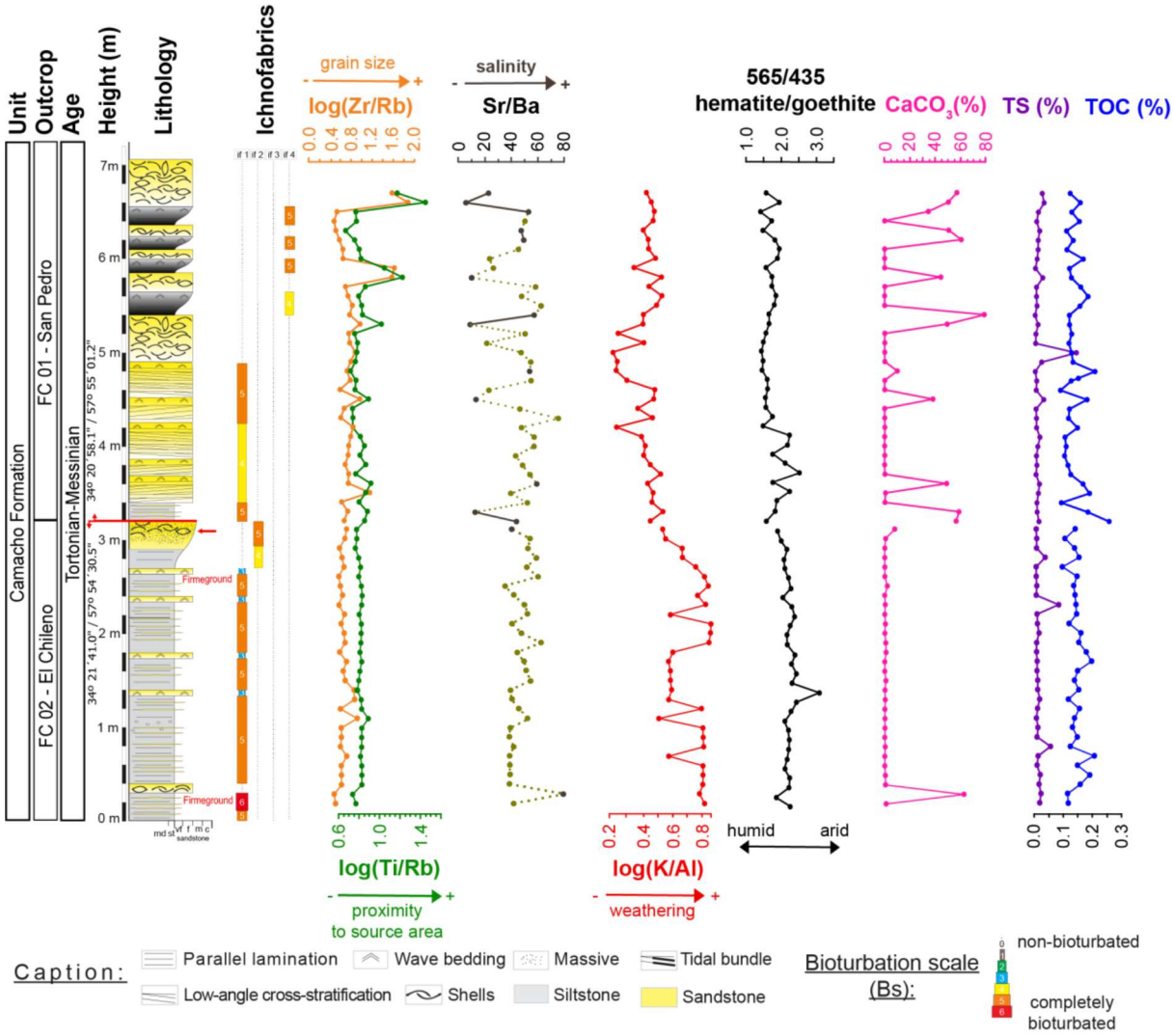

Figure 3. Composite section (outcrops FC01 and FC02) of the Camacho Formation and discussed paleoenvironmental proxies: log(Zr/Rb), log(Ti/Rb), Sr/Ba, log(K/Al), hematite/goethite (565/435 spectral bands) ratio, $CaCO_3$(%), TS (%), and TOC (%). Red horizontal line marks the correlation tie point between sections FC01 and FC02; black points in the Sr/Ba curve mark samples with high carbonate content. For ichnofabric composition, see section 4.1; note that If.3 does not occur in the composite section, but is restricted to the uppermost FC02 section (supplementary Fig. S2). Bioturbation scale based on Reineck (1963).

4. Results

4.1. Sedimentology, facies, and ichnofabrics

The deposits of the Camacho Formation exposed in the studied sections are chiefly composed of highly bioturbated, carbonate-cemented siltstone and fine-grained sandstone, locally interbedded with shell beds and oyster banks (Fig. 2D, E and 4A, B). The abundance of carbonate cement and invertebrate trace and body fossils, and the thicknesses of the shell beds (except the uppermost one), decrease toward the top of the succession and disappear completely in the coarse-grained deposits that overlie the studied sections (Fig. 2F). These coarse-grained strata correspond to Quaternary deposits and were not included in our study (S.A. Martínez, pers. comm.).

The basal deposits at the El Chileno section (FC02; Figure 3; Supplementary Figure S1) are represented by a ~1 m-thick package of highly-bioturbated sandy siltstone interbedded with an oyster bank (Fig. 4A). *Thalassinoides* dominates the trace fossil assemblage, that also contains *Bichordites* (*Laminites* preservation, see Uchman, 1995), *Cylindrichnus*, *Maiakarichnus*, *Ophiomorpha*, *Palaeophycus*, *Planolites*, *Rhizocorallium*, *Rosselia*, and *Siphonichnus*. This trace fossil assemblage characterizes the ichnofabric type 1 (If.1) (Fig. 4C), which was produced chiefly in softgounds, and is pervasive throughout the basal deposits, representing a moderate to high bioturbation intensity. The oyster shells are whole and occur in clusters, some serving as substrate to others (positive taphonomic feedback sensu Kidwell and Jablonski, 1983). These taphonomical signatures suggest autochthonous preservation and indicate the development of beach rocks along the paleo-shoreline. Although the trace fossil assemblage indicates colonization of softgrounds, *Thalassinoides* with sharp borders and filled with coarser-grained sand occur in the sandy siltstone beds that characterize the upper portion of this package, indicating colonization of firmgrounds (e.g., Pemberton et al., 1984; Villegas-Martín et al., 2019). A carbonate-rich bed occurs on top of this basal package. The presence of stratigraphic levels that indicate originally shallow, dewatered or

cemented substrates interbedded with the sandy siltstone deposits suggests the occurrence of a shoaling upward cycle.

The basal sedimentary package is covered by fine-grained heterolithic beds composed of very fine-grained sandstone, siltstone, and claystone. These deposits are organized into four cycles each capped by fine-grained sandstone with wave bedding (Fig. 2F). These cycles vary in thickness from 0.3 to 0.6 m and show a coarsening and thickening-upward trend. Trace fossil content and abundance are similar to the observed in the basal package. Disarticulated mollusk shells and shell fragments occur at the top of the second and the fourth cycles with a chaotic distribution, mostly dispersed but densely packed locally. Sharp-walled burrows passively infilled by rhythmic sedimentation (tubular tidalites, Gingras and Zonneveld, 2015) descend from the top of this heterolithic package, indicating firmground colonization and tidal influence. These features suggest the maintenance of the shoaling upward trend observed in the basal package.

The heterolithic beds are capped by a 0.5 m-thick package composed of a mudstone basal layer that grades upward to very fine to fine-grained sandstone. Vertical burrows of the ichnogenus *Siphonichnus*, with external diameter varying from 3.0 to 6.0 cm and forming tubular tidalites (e.g., Gingras et al., 2012; Wetzel et al., 2014), are abundant in the sandy layers, and compose the type 2 ichnofabric (If.2) (Fig. 4D). Dispersed, disarticulated, and chaotically disposed mollusk shells also occur, becoming more abundant and fragmented towards the top of this package. These deposits are overlaid by a 1.3 m-thick package of fine-grained sandstone beds that characterize the top of the El Chileno section (FC02) (not included in the composite section) (Fig. 2G). The sandstone beds are gently lenticular, forming a quasi-tabular geometry, and show low-angle trough cross-stratification, wavy bedding, swalley cross-stratification, and, locally, hummocky cross-stratification (Fig.2H and I). Whole and fragmented mollusk shells are abundant in these beds, occurring chaotically disposed into the beds and forming shell pavements on bed tops. Trace fossils are less

abundant than body fossils and are represented mostly by *Maiakarichnus, Ophiomorpha*, and *Thalassinoides* (type 3 ichnofabric, If.3; Fig. 4E).

These sandy beds characterize the base of the San Pedro section (FC01; Fig. 3; supplementary Fig. S2), with a thickness of 1.5 m, and showing highly-bioturbated fine-grained deposits interbedded with the sandy beds (Fig. 4G). Bioturbation is moderate in the sandy beds, high in the fine-grained deposits, and represented by two distinct ichnofabrics. The ichnofabric preserved in the sandy beds is dominated by *Ophiomorpha* and *Maiakarichnus*, showing also *Bichordites* (*Laminites* preservation), *Cylindrichnus*, *Palaeophycus*, *Thalassinoides*, and possibly *Schaubcylindrichnus*, configuring a more diverse variation of If.3 with moderated to high bioturbation intensity (BI 4-5) (see supplementary Fig. S1 – note that If.3 only occur in the uppermost San Pedro outcrop and basal El Chileno outcrop, thus, those intervals were not included in the composite section). The ichnofabric preserved in the fine-grained deposits is similar in composition to that observed in the basal beds of the El Chileno section, characterizing the If.1. A ~0.5 m-thick shell bed overlays the sandy beds, forming laterally disposed lenses composed of amalgamated shell pavements, rich in carbonate cement. This shell bed shows a discrete wave bedding. The fine-grained heterolithic deposits occur at the top of the shell bed, interbedded with fine-grained sandstone lenses with wave bedding. Bioturbation is still high, but *Ophiomorpha* and *Thalassinoides* are virtually absent. *Siphonichnus* and *Bichordites* (*Laminites* preservation) are the most frequent burrows in the type 4 (If.4) ichnofabric (Fig. 4F), with an average diameter that is smaller when compared with those of the strata below. *Cylindrichnus, Palaeophycus,* and *Planolites* occur subordinated. Bioturbation intensity in If.4 is moderated (Fig. 3). Another shell bed, also containing small-sized echinoids (3 cm in diameter on average), occurs toward the top of the outcrop (Fig. 4H).

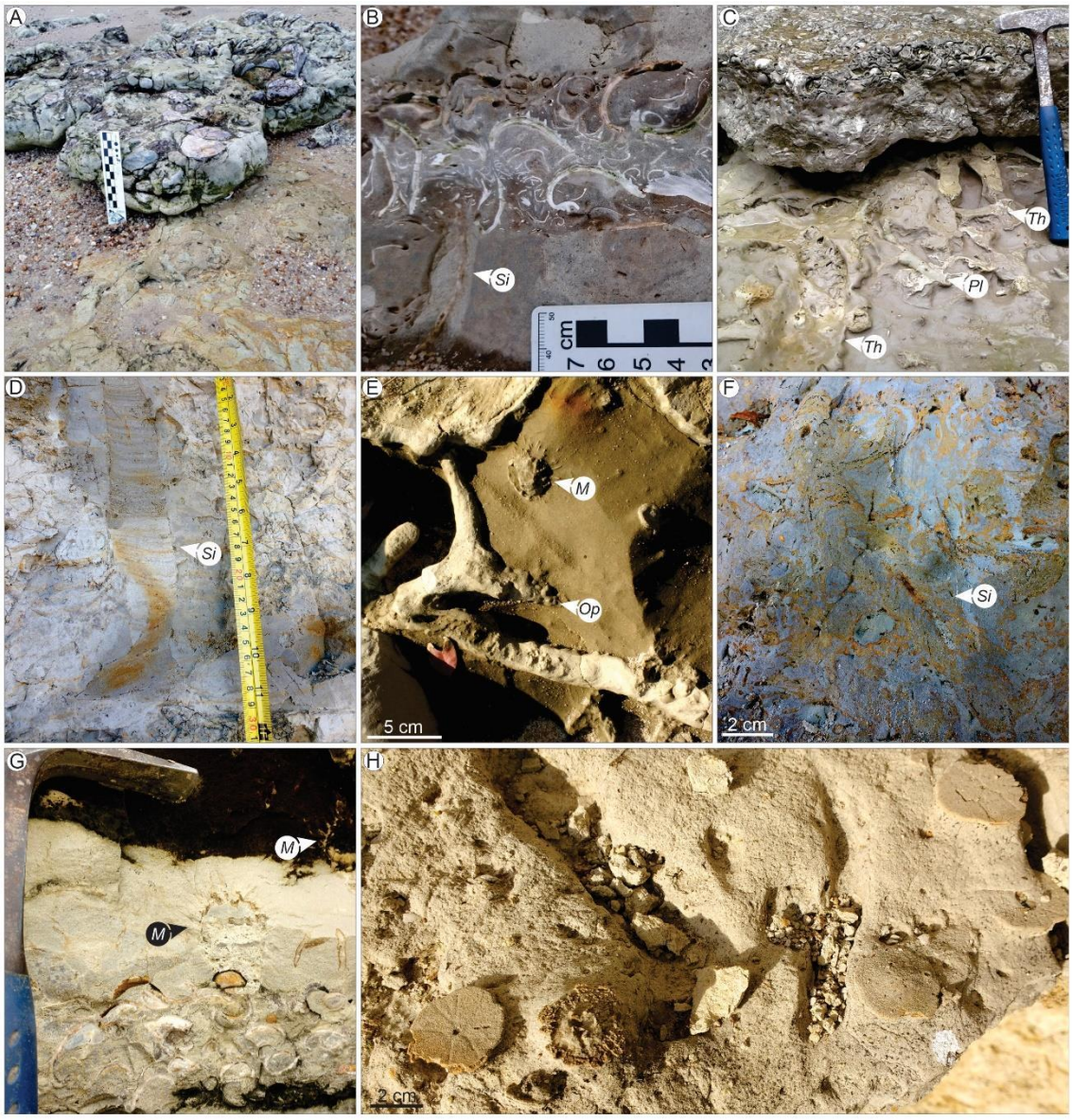

Figure 4. Shell beds and trace fossils from Camacho Formation. A – Basal shell bed composed mainly of *Ostrea* sp. B – Shell beds interbedded with levels bearing trace fossils (*Siphonichnus* - *Si*); C – General view of the type 1 ichnofabric (If.1) with *Thalassinoides* (*Th*) and *Planolites* (*Pl*). D – Type 2 ichnofabric (If.2) with *Siphonichnus* (*Si*) forming tubular tidalites; E – Type 3 ichnofabric (If.3) with *Maiakarichnus* (*M*) and *Ophiomorpha* (*Op*); F – Type 4 ichnofabric (If.4) with small *Siphonichnus* (*Si*); G - Shell beds interbedded among sandy beds with If.3 (*Maiakarichnus* – *M*); H – Bed with whole, convex up small sand-dollars associated with fragmented bivalves and sand-dollars.

4.2. Geochemical proxies

Within the composite section of the Camacho Formation, both log(Zr/Rb) and log(Ti/Rb) show overall increasing upward trends, with relatively higher ratios at the uppermost FC02 outcrop (Fig. 3). Remarkably high log(Zr/Rb) and log(Ti/Rb) ratios occur at 5.8 and 6.6 m within the composite section.

The log(K/Al) ratio presents high values, between 0.6 and 0.9, from the base of the composite section up to 2.6 m (Fig. 3). A decreasing trend occurs between 2.6 and 3.2 m, and log(K/Al) values remained overall bellow 0.5 from 3.2 m to the top of the studied interval (Fig. 3).

The Sr/Ba ratio depicts constant and relatively high values (usually oscillating between 35 and 60) from the base of the composite section to 3.2 m (Fig. 3). This interval is followed by increasingly more pronounced Sr/Ba drops (below 30) between 3.2 and 6.8 m (Fig. 3).

Carbonate content is overall low in the studied succession, with values >40% restricted to the levels described as shell beds (Fig. 3). These stratigraphic levels characterized by increased carbonate content occur dominantly above 3.2 m within the composite section. TOC and TS contents are negligible throughout the studied succession (Fig. 3).

4.3. Spectral reflectance of sediments

All analyzed samples display similar reflectance spectra, but we defined two spectral groups, based on the most pronounced absorption features observed (mean values for each group are plotted in Fig. 5). Group A (52 samples) shows an absorption feature centered at 2200 nm that is related to montmorillonite. Group B (14 samples) also displays this feature at 2200 nm, but additionally presents a diagnostic feature centered at 2320 nm, which is related to carbonate minerals. This implies that clay minerals occur throughout the studied succession

of the Camacho Formation, whereas samples of group B represent mostly shell beds and are also characterized by increased carbonate content.

Both groups display the same spectral pattern in the visible to the near-infrared region (VNIR; 0.35–1.0 µm) with weak absorptions related to Fe minerals. Giosan et al. (2002) and Clift (2006) have used the visible spectral bands to estimate the relative abundances of hematite and goethite, using the 565 nm band to account for hematite and the 435 nm band for goethite. We calculated the hematite/goethite ratio (Fig. 3) using the spectral bands at 564.8 nm for hematite and at 434.6 nm to goethite. The vertical dotted lines in Fig. 5 indicate the position of these bands in nanometers. The hematite/goethite ratio presents overall high values (averaging ~1.7) from the base of the composite section up to ~4 m (Fig. 2). From 4 m to 6.8 m, hematite/goethite ratio shifts to relatively low values, averaging ~1.4 (Fig. 3).

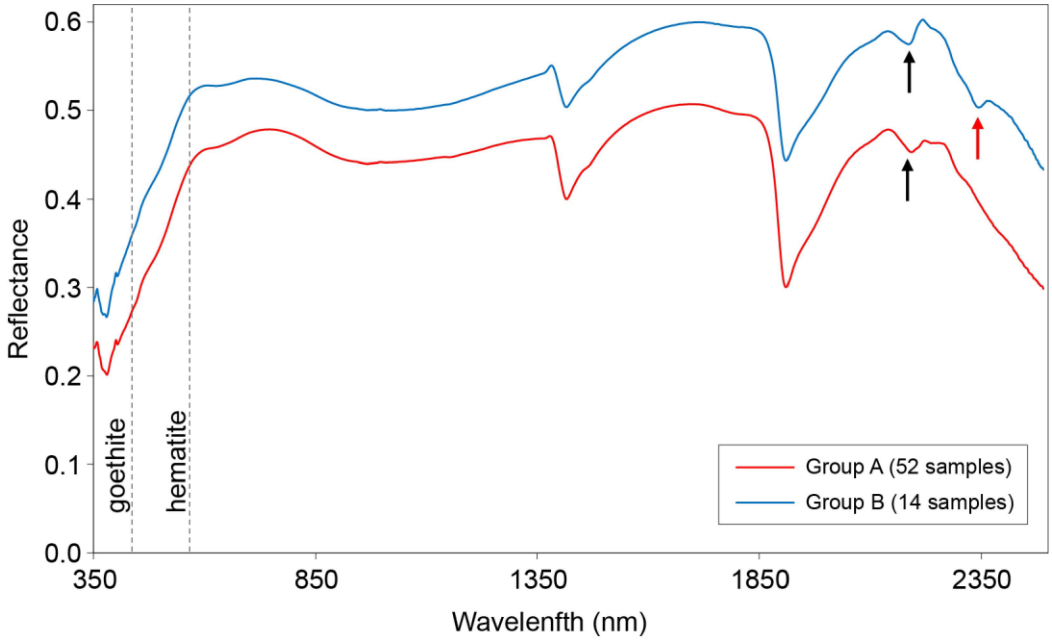

Figure 5. Mean spectral reflectance for groups of samples A and B. Black arrow: montmorillonite absorption feature; red arrow: carbonates absorption feature; vertical dotted lines: position of the goethite (434.6 nm) and hematite (564.8 nm) spectral bands.

5. Discussion

5.1. Paleoenvironmental evolution

The log(Zr/Rb) and log(Ti/Rb) elemental ratios are interpreted as indicative of changes in the grain size and density of the terrigenous components, respectively, thus making it possible to infer distance from the source area, sea level changes, among other processes (e.g., Spofforth et al., 2008; Beil et al., 2018). These inferences are possible because the elements Zr and Ti are usually enriched in heavy and weathering-resistant minerals, such as zircon and titanite (e.g., Calvert and Pedersen, 2007). On the other hand, Rb mainly occurs in weathering-produced aluminosilicates (clays), which are easily transported to relatively distal depositional sites (Rothwell et. al., 2006; Calvert and Pedersen, 2007). Thus, the rates of change in log(Zr/Rb) and log(Ti/Rb) can be applied as proxies for changes in sea level and proximity to the source area (e.g., Spofforth et al., 2008; Beil et al., 2018). At the composite section of the Camacho Formation, log(Zr/Rb) and log(Ti/Rb) depict overall increasing-upward trends (Fig. 3). These trends suggest an overall shallowing-upward trend, with relatively proximal (closer to the sediment sources) conditions likely recorded by the uppermost strata of the Camacho Formation.

The log(K/Al) elemental ratio is generally interpreted as a proxy for the mineralogical composition of the clay associations (e.g., Weaver, 1967, 1989; Niebuhr, 2005; Beil et al. 2018), since K is preferentially delivered to marine sediments in the structure of illite and Al is predominant in kaolinite. Illite is formed at source areas under relatively dry climate conditions, whereas intense chemical weathering in the source areas mostly leads to the formation of kaolinite (Weaver, 1967, 1989; Niebuhr, 2005). The high log(K/Al) values from the base of our composite section up to ~2.5 m (Fig. 2) suggest that this part of the section records relatively dry paleoclimate conditions. Conversely, low log(K/Al), in the order of 0.5, recorded between 3.2 m and 7.2 m indicates intensified chemical weathering under more humid climate conditions at the source areas.

The formation of hematite and goethite during silicate weathering occurs under different climate conditions; hematite is preferentially formed under warm and dry conditions, whereas cold and wet climates lead to the preferential formation of goethite (Schwertmann and Murad, 1983; Cudahy and Ramanaidou 1997; Zhang et al., 2007). Therefore, spectral analyses of iron oxide/oxyhydroxide (hematite (α-Fe2O3) and goethite (α-FeOOH) minerals, which are usually found in sediments and soils, are used as reliable precipitation proxies (Zhang et al., 2007). The hematite/goethite ratio at our composite section presents overall low values above 2.5 m (Fig. 3), suggesting that relatively dry climate conditions prevailed below this stratigraphical level, while strata above recorded wetter climates. The hematite/goethite record thus supports our interpretation based on the log(K/Al) ratio, of more humid climate conditions and enhanced chemical weathering recorded in the uppermost interval of the composite section of the Camacho Formation.

The Sr/Ba ratio can be applied as a paleosalinity proxy in fine-grained sediments (Chen et al., 1997; Ye et al., 2016; Zhang et al., 2007). Strontium presents higher concentrations in sea water, whereas Ba is relatively enriched in brackish and fresh waters; both elements are adsorbed by the structure of silt and clay particles during deposition (Bors et al., 1997; Wei and Algeo 2019). The Sr/Ba ratio presents constantly high values from 0 to 3.2 m at the Camacho Formation composite section; from this level upward, the Sr/Ba record depicts a series of consecutive drops (Fig. 3). Therefore, we can suggest that the strata composing the lowermost 3.2 m of our composite section were deposited under normal marine water salinity (>0.5 Sr/Ba ratio). Above this level, strata were deposited under an increased influence of pulsed freshwater discharge, which is also consistent with the onset of more humid climate conditions.

Besides adsorption by fine-grained sediments, Sr can be incorporated in carbonates, possibly biasing the interpretation of Sr/Ba and a peleosalinity proxy (Wei and Algeo, 2019). To evaluate a possible bounding of Sr to carbonates, we plotted Sr/Ba versus $CaCO_3$ content

(Fig. 6), as proposed by Wei and Algeo (2019). These approach does not show a clear response of Sr/Ba to $CaCO_3$ content, possibly with the exception of one sample (marked in yellow in Fig. 6) that was disregarded from the paleosalinity interpretation.

The presence of exclusively marine trace fossils in the studied sedimentary succession of the Camacho Formation, and body fossils in the fossil concentrations, combined with sedimentary facies, suggest sedimentation in a shallow marine environment, above the fair-weather base and affected by tides and storm surges. This scenario has been previously inferred for the Camacho Formation (e.g., Sprechmann et al., 2000; Verde, 2002; Ugalde-Peralta, 2019) and is herein supported by our multi-proxy approach. Sulfur content and TOC show negligible concentrations throughout the composite section of the Camacho Formation (Fig. 3), suggesting that deposition occurred under the influence of well oxygenated bottom waters (e.g., Calvert and Pedersen 2007). This inference is further supported by the occurrence of abundant and relatively diverse trace fossils produced by benthic organisms in the composite section of the Camacho Formation. The reducing ichnodiversity and intensity of bioturbation towards the top in the analyzed succession is probably a response to the environmental stresses caused by increasing continental input into the marine settings and salinity reduction/fluctuations (e.g., Pemberton et al., 2001; Buatois et al., 2005). However, the possibility that this change in the ichnoassemblage structure could be also triggered by changing climate conditions cannot be discarded.

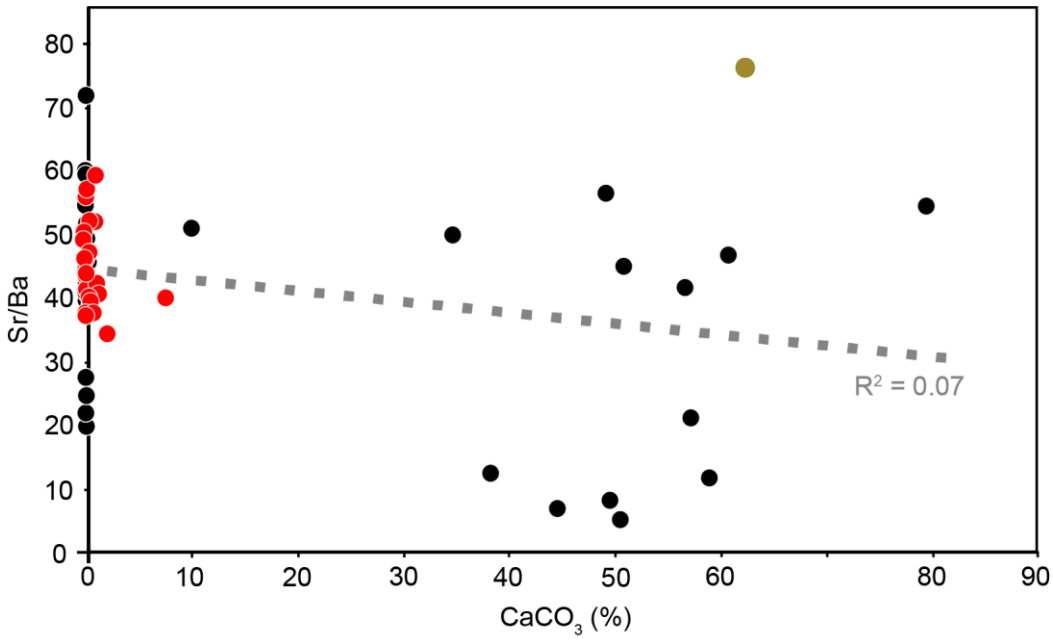

Figure 6. Comparison of Sr/Ba and $CaCO_3$ content within the composite section of the Camacho Formation. The yellow point represents the only sample disregarded from the paleosalinity interpretation due to a possible positive correlation between Sr/Ba and $CaCO_3$ content. Black points are samples from the FC01 outcrop, and red points represent samples from the FC02 outcrop.

5.2. Possible links to global climate changes

In order to compare our paleoenvironmental interpretations for the Camacho Formation with global paleoclimatic events recognized elsewhere, we must first consider an absolute age for the studied succession. Here, we assume that the Tortonian-Messinian $^{87}Sr/^{86}Sr$ average age of 6.6 Ma (maximum age of 7.2 Ma and minimum age of 6.0 Ma; del Río et al., 2018) for the Camacho Formation is the most cautious choice. This $^{87}Sr/^{86}Sr$ measurement was performed on the marine pectinid mollusk *Aequipecten paranensis*, likely recording global trends in the seawater $^{87}Sr/^{86}Sr$ signature. Furthermore, this age estimate agrees well with the most up to date biostratigraphic review for the Camacho Formation by Perea et al. (2020). We refrain from using the Burdigalian ages based on $^{87}Sr/^{86}Sr$ dating of brackish water ostreids by Sprechman et al. (2010), since ostreid $^{87}Sr/^{86}Sr$ ratios could be

more easily affected by diagenesis resulting in significantly older age estimates, as reported by Scasso et al. (2001) for late Miocene shallow-marine strata from Argentina.

Holbourn et al. (2018) identified a high latitude cooling/ice volume expansion event between 7.2 and 7.0 Ma (Fig. 7), which is depicted by a benthic foraminiferal stable oxygen isotope record ($\delta^{18}O$) at Ocean Drilling Program (ODP) Site 1146 (South China Sea). This high latitude cooling event also correlates with the onset of a long-term sea level fall between 7.4 and 6.5 Ma (Fig. 7), as recorded at Pacific Ocean Sites (Miller et al., 2020). Considering the age span of 7.2 to 6.0 Ma proposed by del Río et al. (2018) for the Camacho Formation, the shallowing upward trend recorded in the composite section studied herein could be related to this late Miocene cooling/ice volume expansion event, and its associated sea level fall. In fact, the average age of 6.6 Ma for the Camacho Formation (del Río et al., 2018) correlates well with peak sea level fall in the reconstruction of Miller et al. (2020). We cannot, however, rule out an additional local tectonic influence on the shallowing upward trend recorded by the Camacho Formation, since several areas of eastern South America underwent considerable dynamic uplift during the Neogene, particularly since the Late Miocene (e.g., Tello Saenz et al., 2003; Guillaume et al., 2009; Oliveira et al., 2016; Rodriguez Tribaldos et al., 2017; Klöcking et al., 2020).

Our proxy records at the Camacho Formation also allow to draw some inferences regarding the regional hydroclimate over mid latitudes of South America during the late Miocene. The sea level fall recorded by our composite section was coupled to the establishment of a more humid climatic regime, recorded by the uppermost strata of the Camacho Formation composite section (see section 7.1). This interpretation is supported by the record of *Cyonasua* mammals (Soibelzon et al., 2019) and mammalian bones bioeroded by sarcosaprophagous insects (Perea et al., 2020), which converges to the interpretation of increased aridity in the San Pedro Member of the Camacho Formation (base of the studied succession). This pattern contrasts with the strengthening of the Asian winter (dry) monsoon,

which followed the onset of high latitude cooling after ~7.2 Ma (Holbourn et al., 2018). Such differences could be related to latitudinal migrations of climate belts and atmospheric Hadley circulation changes, associated with changing latitudinal thermal gradients (e.g., Brierley et al., 2009), which may have led to different regional trends in mid latitudes over South America and southern Asia during the late Miocene.

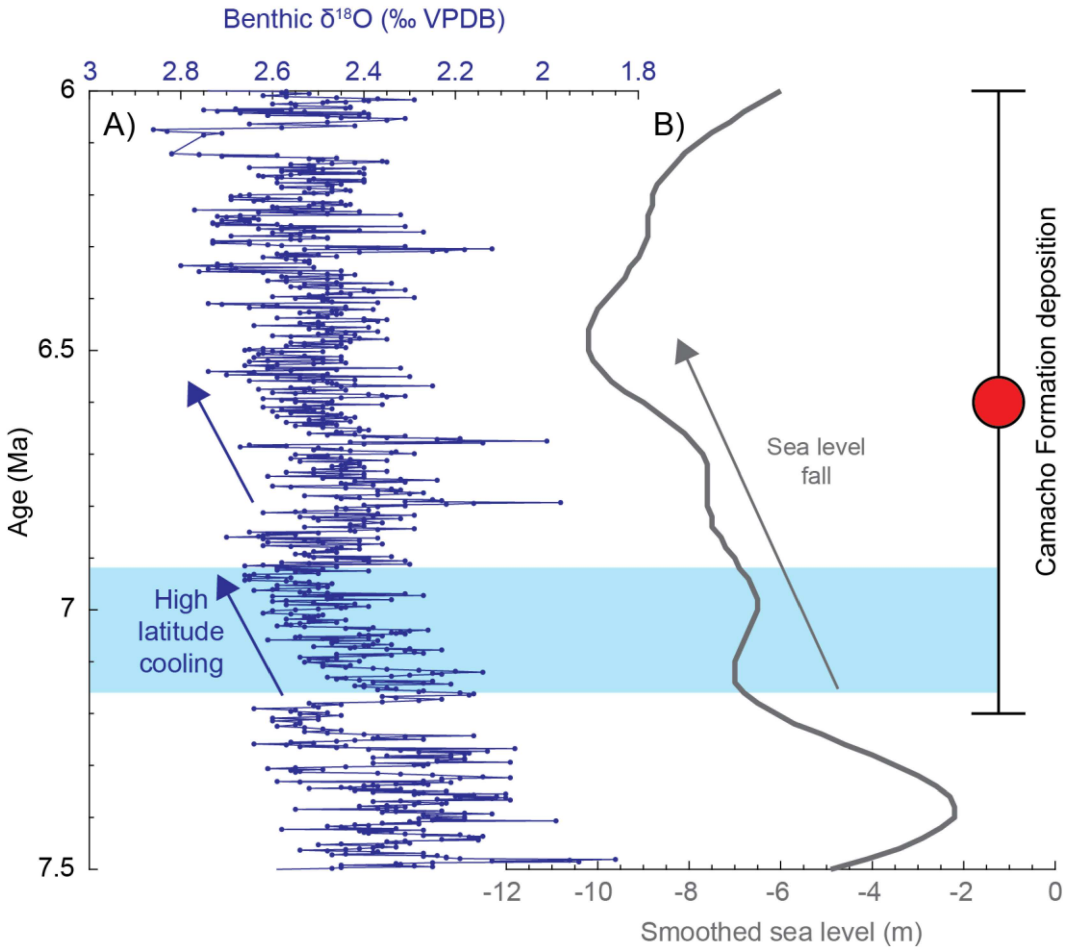

Figure 7. Late Miocene (7.5 to 6.0 Ma) climate and sea level changes. A) Benthic stable oxygen ($\delta^{18}O$) isotope record at Ocean Drilling Program (ODP) Site 1146 (Holbourn et al., 2018), located at the South China Sea. B) Smoothed sea level reconstruction of Miller et al. (2020), calculated in relation to the present sea level. Blue shading and arrows mark the high latitude cooling and/or ice volume expansion event at ~7.2-6.9 Ma (Holbourn et al., 2018) and a subsequent benthic $\delta^{18}O$ increase at ~6.8-6.5 Ma. A late Miocene long-term sea level fall is marked by a gray arrow. The depositional age range for the Camacho Formation suggested by

Del Rio et al. (2018) is presented on the right side of the panel; the red circle marks the average for the Camacho Formation, and minimum and maximum ages are bracketed by an error bar. VPDB: Vienna PeeDee Belemnite scale.

6. Conclusions

High resolution geochemical, sedimentological, and ichnological data from the Camacho Formation, cropping out in southwestern Uruguay, enables to reconstruct regional paleoenvironmental settings of the late Miocene "Entrerriense Sea". Our data support previous interpretations of deposition in shallow marine environments, with well oxygenated waters, and under the influence of moderate to low energy processes, with deposition affected by tides and storm. Our high-resolution proxy records further depicted a shallowing upward trend in the composite section of the Camacho Formation, which is reinforced by the reducing in ichnodiversity and bioturbation intensity. More proximal conditions, also subjected to a more humid paleoclimate, and increased influence of freshwater input, were recorded by the uppermost strata of the Camacho Formation. Some of these patterns were probably linked to high-latitude cooling events and associated sea level fall that occurred during the late Miocene. Additionally, the regional hydroclimate recorded by the Camacho Formation was likely affected by climate belt displacements that probably followed high-latitude cooling.

7. Acknowledgments

We thank F. L. Souza, and M. D. R. Bruno, for assistance during field work. G. E. R. Racolte is thanked for assistance with spectral reflectance analysis and we thank VizLab (UNISINOS University) for providing the spectroradiometer used in this study. We would also like to thank the Faculdad de Ciencias da Universidad de la República, Uruguay, for field work assistance while collecting the studied samples. We are also grateful to the staff at itt OCEANEON (UNISINOS University) for assisting with geochemical analyses, especially M.

G. Silva and L. R. C. Duarte. RGN thanks to the Brazilian National Council for the Development of Scientific and Technological Research (CNPq) for grants 424237-2018-0 and 310377/2019-6. This work is part of the project "*Impactos de mudanças climáticas na distribuição da bioturbação em ambientes marinhos rasos no Atlântico Sul*".

8. References

Aceñolaza, F.G., 1976. Consideraciones bioestratigráficas sobre el Terciario marino de Paraná y alrededores. Acta Geol. Lilloana 13 (2), 91–107 Tucumán.

Aceñolaza, F.G., 2000. La Formación Paraná (Mioceno medio): estratigrafía, distribución regional y unidades equivalentes. In: In: Aceñolaza, F.G., Herbst, R. (Eds.), El Neógeno de Argentina, vol. 14. Serie Correlación Geológica, pp. 9–27.

Angulo, R., Casamiquela, R., 1982. Estudio estratigráfico de las unidades aflorantes en los acantilados de la costa norte del golfo San Matías (Río Negro y extremo austral de Buenos Aires) entre los meridianos 62 30' y 64 30'. Mundo Ameghiniano 2, 20–73.

Arthur, M.A., Schlanger, S.O., 1979. Cretaceous "Oceanic Anoxic Events" as causal factors in development of reef-reservoired giant oil fields. The American Association of Petroleum Geologists Bulletin, 63, 870–885.

Beil, S., Kuhnt, W., Holbourn, A.E., Aquit, M., Flögel, S., Chellai, E.H., Jabour, H., 2018. New insights into Cenomanian paleoceanography and climate evolution from the Tarfaya Basin, southern Morocco. Cretaceous Research, 84, 451–473.

Brierley, C. M., Fedorov, A. V., Liu, Z., Herbert, T. D., Lawrence, K. T., & LaRiviere, J. P., 2009. Greatly expanded tropical warm pool and weakened Hadley circulation in the early Pliocene. Science, 323(5922), 1714-1718.

Bors, J., Gorny A., Dultz, S., 1997. Iodide, Caesium and Strontium adsorption by organophilic vermiculite. Clay Miner., 32, 21–28.

Buatois, L.A., Gingras, M.K., MacEachern, J., Mángano, M.G., Zonneveld, J.-P., Pemberton, S.G., Netto, R.G., Martin, A., 2005. Colonization of brackish-water systems through time: Evidence from the trace-fossil record. Palaios 20, 321–347. doi:10.2110/palo.2004.p04-32

Calvert, S.E., Pedersen, T.F., 2007. Chapter fourteen elemental proxies for palaeoclimatic and palaeoceanographic variability in marine sediments: interpretation and application. Developments in Marine Geology, 1, 567–644. doi:10.1016/S1572-5480(07)01019-6.

Caorsi, J.H., Goñi, J.C., 1958. Geología uruguaya. Bol. Inst. Geol. Uruguay., 37, l–73.

Chen Z.Y., Chen Z.L., Zhang, W.G., 1997. Quaternary stratigraphy and trace-element indices of the Yangtze Delta, Eastern China, with special reference to marine transgressions. Quat. Res., 47, 181–191.

Clark, R.N., Swayze, G.A., Wise, R., Livo, E., Hoefen, T., Kokaly, R., Sutley, S.J., 2007. USGS digital spectral library splib06a, Data Series 231, U.S. Geol. Surv, Reston, Va. (Available at http://speclab.cr.usgs.gov/ spectral.lib06).

Clift, P.D., 2006. Controls on the erosion of Cenozoic Asia and the flux of clastic sediment to the ocean. Earth and Planetary Science Letters, 241, 571–580. doi:10.1016/j.epsl.2005.11.028

Closs, D., Madeira, M.L., 1968. Cenozoic Foraminifera from the Chuy drill hole, northern Uruguay. Ameghiniana, 5, 229–246.

Cudahy, T.J., Ramanaidou, E.R., 1997. Measurement of the hematite:goethite ratio using field visible and near- infrared reflectance spectrometry in channel iron deposits, Western Australia. Australian Journal of Earth Sciences, 44, 411–420.

Darwin, C., 1839. Narrative of the surveying voyages of his Magesty's ships adventure and beagle between the years 1826 and 1836, describing their examination of the Southern shores of South America and the Beagle' s circumnavigation of the Globe, 3. Colburn, London, pp XIV, 615 pp.

Darwin, C., 1846. Geological observations on South America: Being the third part of the geology of the voyage of the Beagle, under the command of Capt. Fitzroy, RN during the years 1832 to 1836, Smith, Elder & Co, London, 65, l279 pp.

del Río, C.J., Martínez, S., McArthur, J., Thirlwall, M., Pérez, L., 2018. Dating late Miocene marine incursions across Argentina and Uruguay with Sr-isotope stratigraphy. Journal of South American Earth Sciences, 85, 312–324.

del Río, C.J., Martínez, S., 1998. El Mioceno marino en la Argentina y en el Uruguay. In C. J. del Río (Ed.), Moluscos marinos Miocenos de la Argentina y del Uruguay. Monografías de la Academia Nacional de Ciencias Exactas Físicas y Naturales de Buenos Aires, 15, pp. 5–25.

de Oliveira, C. H. E., Jelinek, A. R., Chemale Jr, F., & Bernet, M., 2016. Evidence of post-Gondwana breakup in Southern Brazilian Shield: Insights from apatite and zircon fission track thermochronology. Tectonophysics, 666, pp. 173-187.

Figueiras, A., Broggi. J., 1971. Estado actual de nuestros conocimientos sobre los moluscos fósiles del Uruguay. Ill (cont.).Com. Soc. Malac. Uruguay, 3, 131–154.

Francis, J.C., l975. Esquema bioestratigráfico regional de la República Oriental del Uruguay. Actas l Congr. Arg. Paleont. Bioest., Tucumán, v. 2, pp. 539–568.

Gingras, M. K., & Zonneveld, J. P., 2015. Tubular tidalites: a biogenic sedimentary structure indicative of tidally influenced sedimentation. Journal of Sedimentary Research, 85, 845-854.

Gingras, M.K., MacEachern, J.A., Dashtgard, S.E., 2012. The potential of trace fossils as tidal indicators in bays and estuaries. Sedimentary Geology, 279, 97–106.

Giosan, L., Flood, R.D., Grutzner, J., Mudie, P., 2002. Paleoceanographic significance of sediment color on western North Atlantic drifts: II Late Pliocene–Pleistocene sedimentation. Marine Geology, 189, 43–61.

Grygar, T.M., Mach, K., Martínez, M., 2019. Checklist for the use of potassium concentrations in siliciclastic sediments as paleoenvironmental archives. Sedimentary Geology, 382, 75–84.

Goñi, J.C., Hoffstetter, R., 1964. Uruguay. CNRS, Paris, Lexique Stratigr. lnternat., 5 Amér. Latine (9a), pp. 1–202.

Goso, H., Bossi, J.C., 1966. Cenozoico. ln Bossi, J.C. (Ed.), Geología del Uruguay. Univ. República, Montevideo, pp. 259 –305.

Guillaume, B., Martinod, J., Husson, L., Roddaz, M., Riquelme, R., 2009. Neogene uplift of central eastern Patagonia: Dynamic response to active spreading ridge subduction?, Tectonics, 28, pp. 1-19. https://doi:10.1029/2008TC002324.

Haller, M.J., 1978. Estratigrafía de la región al poniente de Puerto Madryn, provincia del Chubut, República Argentina. 7º Congreso Geológico Argentino (Buenos Aires). Actas 1, 285–297.

Herbert, T.D., Lawrence, K. T., Tzanova, A., Peterson, L. C., Caballero-Gill, R., & Kelly, C. S., 2016. Late Miocene global cooling and the rise of modern ecosystems. Nat. Geosci. 9, 843–847.

Herbst. R., Zabert, L.L., l979. Nota sobre la microfauna de la Formación Camacho (Mioceno Superior) del Uruguay occidental. FACENA, 3, 5–17.

Herbst, R., Zabert, L.L., 1987. Microfauna de la Fm. Paraná (Mioceno Superior) de la Cuenca Chaco-Paranense (Argentina). FACENA, 7, l65–206.

Holler, F.J., Skoog, D.A., Crouch, S.R., 2009. Princípios de Análise Instrumental. Bookman, pp. 323–327.

Holbourn, A.E., Kuhnt, W., Clemens, S.C., Kochhann, K.G., Jöhnck, J., Lübbers, J., Andersen, N., 2018. Late Miocene climate cooling and intensification of southeast Asian winter monsoon. Nature Communications, 9, 1–13.

Kidwell, S.M., Jablonski, D., 1983. Taphonomic feedback: Ecological consequences of shell accumulation. In: Tevesz, M. J. S., McCall, P.L. (Eds.), Biotic Interactions in Recent and Fossil Benthic Communities. Plenum Press, New York, pp. 195–248.

Klöcking, M., Hoggard, M. J., Tribaldos, V. R., Richards, F. D., Guimarães, A. R., Maclennan, J., & White, N. J., 2020. A tale of two domes: Neogene to recent volcanism and dynamic uplift of northeast Brazil and southwest Africa. Earth and Planetary Science Letters, 547, 116464.

Köhler, C.M., Heslop, D., Krijgsman, W., Dekkers, M.J., 2010. Late Miocene paleoenvironmental changes in North Africa and the Mediterranean recorded by geochemical proxies (Monte Gibliscemi section, Sicily). Palaeogeography, Palaeoclimatology, Palaeoecology, 285, 66–73.

Kraglievich, L., 1928. Apuntes para la geología y paleontología de la República Oriental del Uruguay. Rev. Soc. Amigos Arqueol., 2, pp. 56l.

Lambert, R., 1940. Observaciones geológicas en la región sud-oeste del Uruguay (Departamentos de Soriano y Colonia). Rev. Ingeniería, 33, 377–385.

Marengo, H.G., 2015. Neogene micropaleontology and stratigraphy of Argentina. The Chaco - paranense Basin and the Península de Valdés. Springer Briefs in Earth Systems Sciences. South America and the Southern Hemisphere 218 10.1007/978-3-319-12814-6.

Marshall, L., Hoffstetter, R., Pascual, R., 1983. Mammals and Stratigraphy: Geochronology of the continental Mammal-bearing Tertiary of South America. Montpellier, Palaeovertebrata, Mém. Ext., 1–90 pp.

Martínez, S., 1994. Bioestratigrafía (invertebrados) de la Formación Camacho (Mioceno, Uruguay). Ph.D. Thesis. Facultad de Ciencias Exactas y Naturales, Universidad de Buenos Aires). Available at https://bibliotecadigital.exactas.uba.ar/download/tesis/tesis_n2722_MartinezChiappara.pdf

Miller, K.G., Browning, J.V., Schmelz, W.J., Kopp, R.E., Mountain, G.S., Wright, J.D., 2020. Cenozoic sea-level and cryospheric evolution from deep-sea geochemical and continental margin records. Science Advances, 6, eaaz1346.

Mones, A., l979. Terciario del Uruguay. Síntesis Geo-Paleontológica. Rev. Fac. Hum. Cienc. (Cienc. Tierra), 1, l–27.

Niebuhr, B., 2005. Geochemistry and time-series analyses of orbitally forced Upper Cretaceous marlelimestone rhythmites (Lehrte West Syncline, northern Germany). Geological Magazine, 142, 31–55. doi:10.1017/S0016756804009999.

Palacio, J.L., Sánchez, J.L.; Schilling, M., 2016. Patrimonio geológico y su conservación en América Latina: Situación y perspectivas nacionales. Instituto de Geografía, Universidad Nacional Autónoma de México, pp. 265.

Pere, D., Ubilla, M., 1989. Selacífauna del Mioceno Superior del Uruguay. Bol. Soc. Zool. Uruguay (2a Epoca), 5, 11–12.

Perea, D., Ubilla, M., 1990. Los Selacios (Chondrichthyes) de la Fm. Camacho (Mioceno Sup., Uruguay). Rev. Soc. Urug. Geol., 2, 5–13.

Perea, D., Martínez, S., 2004. Estratigrafía del Mioceno–Pleistoceno en el litoral sur-oeste de Uruguay. Cuencas sedimentarias de Uruguay, Geología, Paleontología y Recursos Naturales, Cenozoico. In: Veroslavsky, G., Ubilla, M., Martínez, S. (Eds.), 3 Ediciones DIRAC, Facultad de Ciencias, Montevideo, pp. 105–124.

Perea, D., Gutiérrez, G.D.M., Lorenzo, N., Martínez, S., Piñeiro, G., Lecuona, G.R., Rinderknecht, A., Rojas, A., Ubilla, M., Soto, M., Veroslavsky, G., Verde, M., 2011. Fósiles de Uruguay. DIRAC. cap. 12, pp. 265-276.

Perea, D., Rinderknecht, A., Ubilla, M., Bostelmann, E., & Martínez, S., 2013. Mamíferos y estratigrafía del Neógeno de Uruguay. In D. Brandoni & J. I. Noriega (Eds.), El Neógeno de la Mesopotamia Argentina. Publicación Especial de la Asociación Paleontológica Argentina, 14, 192–206..

Perea, D., Verde, M., Toriño, P., Montenegro, F., Ubilla, M., Manzuetti, A., 2020. A Complex association of invertebrates, vertebrates and trace fossils in the marine Camacho

Formation (Late Miocene of Uruguay): Biostratigraphy and paleoenvironments. Ameghiniana, 57, 266–277.

Pemberton, S.G., Frey, R.W., Walker, R.G., 1984. Probable lobster burrows in the Cardium Formation (Upper Cretaceous) of southern Alberta, Canada, and comments on modern burrowing decapods. Journal of Paleontology 58, 1422–1435.

Pemberton, S.G., Spila, M., Pulham, A.J., Saunders, T., MacEachern, J.A., Robbins, D., Sinclair, I.K. 2001. Ichnology and sedimentology of shallow to marginal marine systems. Geological Association of Canada, Short Course Notes 15, 343 pp.

Reineck, H. E.,1963. Sedimentgefüge im Bereich der südlichen Nordsee.Rodríguez Tribaldos, V., White, N. J., Roberts, G. G., & Hoggard, M. J. (2017). Spatial and temporal uplift history of S outh A merica from calibrated drainage analysis. Geochemistry, Geophysics, Geosystems, 18, pp. 2321-2353.

Rothwell, R.G., Hoogakker, B., Thomson, J., Croudace, I.W., Frenz, M., 2006. Turbidite emplacement on the southern Balearic Abyssal Plain (western Mediterranean Sea) during Marine Isotope Stages 1–3: An application of ITRAX XRF scanning of sediment cores to lithostratigraphic analysis. Geological Society, London, Special Publications, 267, 79–98.

Saenz, C. T., Hackspacher, P. C., Neto, J. H., Iunes, P. J., Guedes, S., Ribeiro, L. F. B., Paulo, S. R., 2003. Recognition of Cretaceous, Paleocene, and Neogene tectonic reactivation through apatite fission-track analysis in Precambrian areas of southeast Brazil: association with the opening of the South Atlantic Ocean. Journal of South American Earth Sciences, 15, 765-774.

Scasso, R.A., McArthur, J.M., del Río, C.J., Martínez, S.A., Thirlwall, M.F., 2001. 87Sr/86Sr late Miocene age of fossil mollusks in the “Entrerriense” of Valdés Peninsula (Chubut, Argentina). J. S. Am. Earth Sci., 14, 319–329.

Scasso, R.A., del Río, C.J., 1987. Ambientes de sedimentación y proveniencia de la secuencia marina del Terciario superior de la península Valdés. Rev. Asoc. Geol. Argent. 42, 291–321.

Schwertmann, U., Murad, E., 1983. Effect of pH on the formation of goethite and hematite from ferrihydrite. Clays Clay Miner., 31, 277–284.

Serra. N., l943. Memoria explicativa del mapa geológico del Departmento de Colonia. Bol. Inst. Geol. Uruguay, 30, 1–50. Montevideo.

Simões, M.G., Torello, F., 2003 Modelo de tafofácies para os moluscos bivalves do Grupo Passa Dois (Formaççoes Serra Alta, Teresina e Corumbataí), Permiano Superior do Paraná, Brasil, Revista Brasileira de Geociências, 33,371–380.

Soibelzon, L.H., Rinderknecht, A., Tarquini, J., Ugalde, R., 2019. First record of fossil procyonid (Mammalia, Carnivora) from Uruguay. Journal of South American Earth Sciences, 92, 368–373.

Spofforth, D.J., Pälike, H., Reen, D., 2008. Paleogene record of elemental concentrations in sediments from the Arctic Ocean obtained by XRF analyses. Paleoceanography, 23, 1, pp. 1-13. doi:10.1029/2007PA001489.

Sprechmann, P., 1978. The paleoecology and palegeography of the Uruguayan coastal area during the Neogene and Quaternary. Zitteliana, 4, 3–72.

Sprechmann, P., 1980. Paleoecología, paleogeografía y estratigrafía de la región costera del Uruguay durante el Neógeno y Cuartario. Actas 2 Congr. Arg. Paleont. Bioest., I Congr. Latinoamer. Paleont., Buenos Aires, v. 3, pp. 237–256.

Sprechmann, P., Gaucher, C., Frei, R., 2010. Identificación del Bur - digaliense (Mioceno temprano) en ostreidos procedentes de afloramientos de la Formación Camacho de Uruguay datados con 87Sr/86Sr. Resúmenes de 10º Congreso Argentino de Paleontología y Bioestrati grafía y 7º Congreso Latinoamericano de Paleontología, pp. 144). La Plata.

Sprechmann, P., Ferrando, A.L., Martínez, S., 2000. Estado actual de los conocimientos sobre la Formación Camacho (Mioceno Medio?–Superior?, Uruguay). In: Aceñolanza, F.G., Herbst, R. (Eds.), El Neógeno de Argentina. INSUGEO, Serie Correlación Geológica, Tucumán, pp. 47–65.

Stax, R., Stein, R., 1993. Long-term changes in the accumulation of organic carbon in Neogene sediments, Ontong Java Plateau. Proceedings of the Ocean Drilling Program, Scientific Results, v. 130, pp. 573–579. doi:10.2973/odp.proc.sr.130. 039.1993.

Teisseire, A., l928. Contribución al estudio de la geología y paleontología de la República Oriental del Uruguay. Región de Colonia. An. Uníversidad, 37, 319–469.

Tzanova, A., Herbert, T.D., Peterson, L., 2015. Cooling Mediterranean Sea surface temperatures during the Late Miocene provide a climate context for evolutionary transitions in Africa and Eurasia. Earth. Planet. Sci. Lett., 419, 71–80.

Uchman, A., 1995. Taxonomy and palaeoecology of flysch trace fossils: The Marnoso arenacea Formation and associated facies (Miocene, Northern Apennines, Italy). Beringeria, 15, 1–115.

Ugalde Peralta, R. A., 2019. Petrografía, quimioestratigrafía y proveniencia sedimentaria de la Formación Camacho (Mioceno), Uruguay. pp. 238.

Verde, M. 2002. Icnología de la Formación Camacho (Mioceno Tardío) del Uruguay. MSc Thesis, Universidad de la República, Montevideo, 124 pp.

Verde, M., Martinez, S. 2004. A new ichnogenus for crustacean trace fossils from the upper Miocene Camacho Formation of Uruguay. Palaeontology, 47, 39–49. doi:10.1111/j.0031-0239.2004.00346.x

Villegas-Martín, J., Ceolin, D., Fauth, G., & Klompmaker, A. A., 2019. A small yet occasional meal: predatory drill holes in Paleocene ostracods from Argentina and methods to infer predation intensity. Palaeontology, 62, 731-756.

Vinadé, M.E. do C., Vinadé, E.R. do C., 2005. Métodos Espectroscópicos de Análise Química. UFSM, Santa Maria, cap. 11, 227-243.

Walther, K., 1931. Sedimentos gelíticos y clastogelíticos del Cretáceo Superior y Terciario uruguayos. Bol. lnst. Geol. Perf., 13, l–l42.

Wahnish, E., 1939. Perforación Riachuelo No.5. Buenos Aires. Perfil geológico y descripción de los fósiles. In: Revista del Centro de Estudiantes de Ciencias Naturales, vol. 2. pp. 141–156.

Weaver, C.E., 1967. Potassium, illite and the ocean. Geochimica et Cosmochimica Acta, 31, 2181–2196. doi:10.1016/0016-7037(67)90060-9.

Weaver, C.E., 1989. Clays, Muds, and Shales. Elsevier. (Vol. 44). Developaents in Sedimentology, pp. 809.

Wei, G., Li, X.H., Liu, Y., Shao, L., Liang, X., 2006. Geochemical record of chemical weathering and monsoon climate change since the early Miocene in the South China Sea. Paleoceanography, 21, pp. 1-11. doi:10.1029/2006PA001300, 2006

Wei, W., Algeo, T.J., 2020. Elemental proxies for paleosalinity analysis of ancient shales and mudrocks. Geochimica et Cosmochimica Acta, 287, 341-366.

Wetzel, A., Carmona, N., Ponce, J., 2014. Tidal sig na ture re corded in burrow fill. Sedimentology, 61, 1198–1210.

Yang, R., Yang, Y., Fang, X., Ruan, X., Galy, A., Ye, C., Han, W., 2019. Late Miocene intensified tectonic uplift and climatic aridification on the northeastern Tibetan Plateau: Evidence from clay mineralogical and geochemical records in the Xining Basin. Geochemistry, Geophysics, Geosystems, 20, 829–851.

Ye, C., Yang, Y., Fang, X., Zhang, W., 2016. Late Eocene clay boron-derived paleosalinity in the Qaidam Basin and its implications for regional tectonics and climate. Sed. Geol., 346, 49–59.

Zhang, Y.G., Ji, J., Balsam, W.L., Liu, L., Chen, J., 2007. High resolution hematite and goethite records from ODP 1143, South China Sea: Co-evolution of monsoonal precipitation and El Niño over the past 600,000 years. Earth and Planetary Science Letters, 264, 136–150.

Journal of South American Earth Science

ONLINE SUPPORTING INFORMATION FOR:

Paleoenvironmental conditions of the late Miocene "Entrerriense" epicontinental sea: A case study of the Camacho Formation, SW Uruguay

Gustavo N. Aumonda, Karlos G. D. Kochhanna, Renata G. Nettoa, Laís V. de Souzab, Daniel Sedorkoc, Rodrigo S. Horodyskia, Flavio N. Almeida Júniord.

a Geology Graduate Program, Unisinos University – Av. Unisinos, 950 – Bairro Cristo Rei, São Leopoldo/RS – Brazil. gustavo.aumond@gmail.com, kkochhann@unisinos.br, nettorg@unisinos.br

b VizGEO Lab, Unisinos University – Av. Unisinos, 950 – Bairro Cristo Rei, São Leopoldo/RS – Brazil. laisvs@unisinos.br

c Labortório de Paleontologia Estratigráfica, Geography Institute, Federal University of Uberlândia. Av. XV de novembro, 501, Boa Vista. Monte Carmelo – MG, 38500-000, Brazil. sedorko@ufu.br

d Department of Earth Science, University of Bergen, Allégaten 41, 5007, Bergen, Norway. Flavio.DeAlmeida@uib.no

Contents of this file: Figures S1 to S3

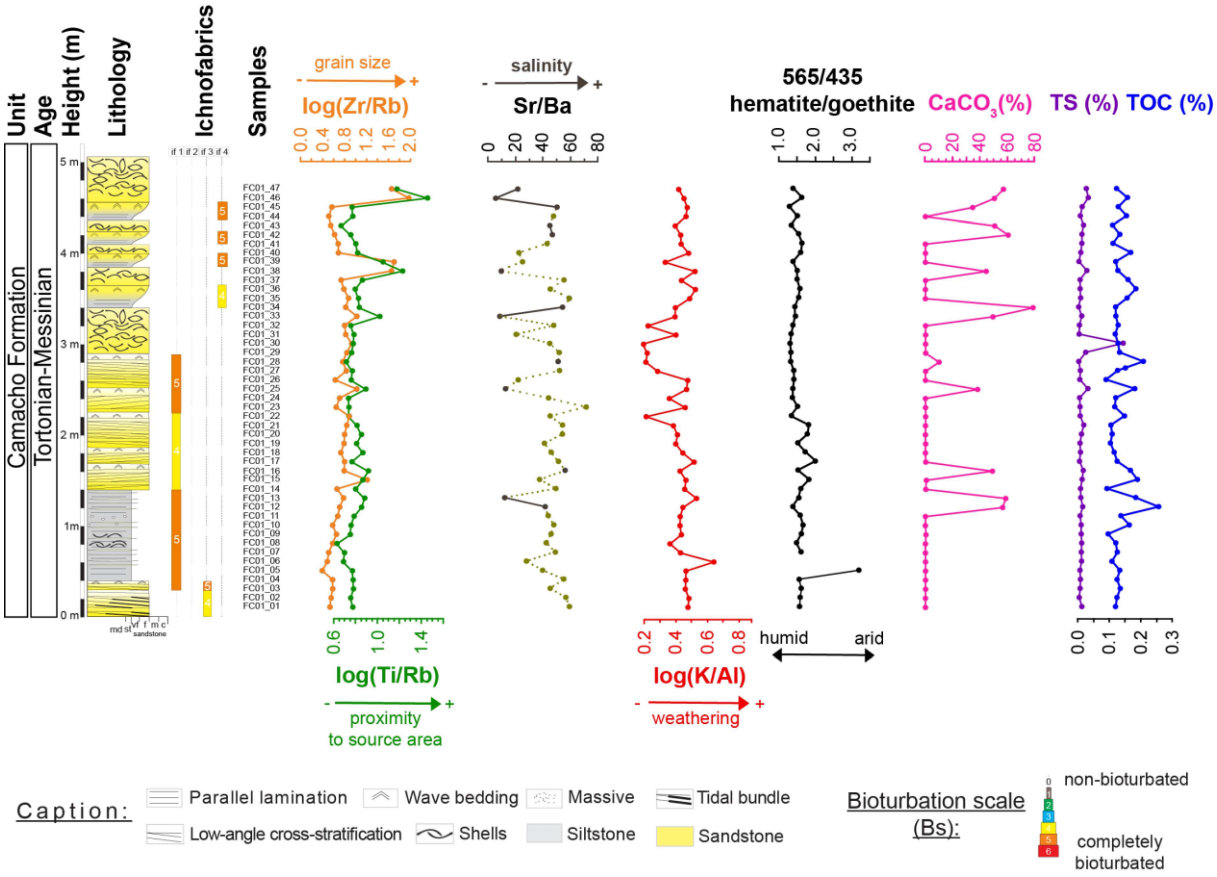

Figure S1. *San Pedro* outcrop (FC01) and discussed paleoenvironmental proxies: log(Zr/Rb), log(Ti/Rb), Sr/Ba, log(K/Al), hematite/goethite (565/435 spectral bands) ratio, $CaCO_3$ (%), TS (%), and TOC (%). Back points in the Sr/Ba curve mark samples with high carbonate content. Ichnofabrics composition and bioturbation intensity as in Fig. 3 and in the main text.

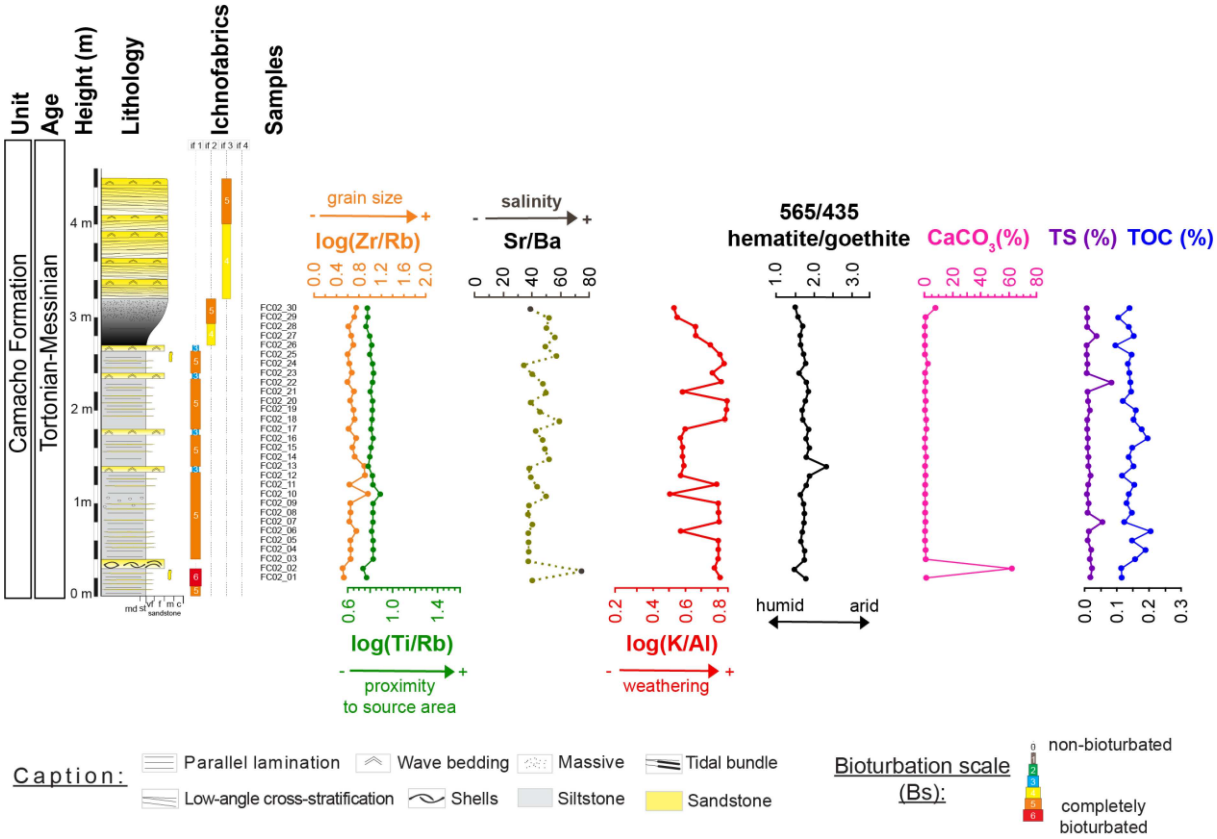

Figure S2. El Chileno outcrop (FC02) and discussed paleoenvironmental proxies: log(Zr/Rb), log(Ti/Rb), Sr/Ba, log(K/Al), hematite/goethite (565/435 spectral bands) ratio, $CaCO_3$ (%), TS (%), and TOC (%). Black points in the Sr/Ba curve mark samples with high carbonate content. Ichnofabrics composition and bioturbation intensity as in Fig. 2 and in the main text.

CONSIDERAÇÕES FINAIS

O desenvolvimento de um estudo multi-*proxy* nos possibilitou contribuir para uma análise de alta resolução das mudanças paleoambientais ocorridas no "Mar Entrerriense" durante o Mioceno tardio, na região sudeste do Uruguai. Interpretações anteriormente apresentadas por diferentes autores(as) (exemplo: Perea and Martínez 2004; Perea et al., 2011; del Rio et al., 2018), de um ambiente marinho raso, de águas bem oxigenadas, de energia moderada a baixa, e de deposição afetada por marés e tempestades, são suportados pelos dados aqui analisados. Adicionalmente, os dados apresentados aqui sugerem uma tendência de raseamento em direção ao topo da seção composta da Formação Camacho, associada a paleoclimas mais úmidos e maior influência do aporte de água doce em direção ao topo da seção estudada. Os padrões sedimentares registrados pela Formação Camacho estão possivelmente relacionados ao resfriamento de altas latitudes e à queda do nível do mar, iniciados há ~7.2 Ma. Entretanto, os padrões do hidroclima regional registrados pela Formação Camacho ainda necessitarão de estudos adicionais para uma melhor compreensão de suas relações com as variações climáticas globais ocorridas durante o Mioceno tardio.

REFERENCES

del Río, C.J., Martínez, S., McArthur, J., Thirlwall, M., Pérez, L., 2018. Dating late Miocene marine incursions across Argentina and Uruguay with Sr-isotope stratigraphy. Journal of South American Earth Sciences, 85, 312–324.

Holbourn, A.E., Kuhnt, W., Clemens, S.C., Kochhann, K.G., Jöhnck, J., Lübbers, J., Andersen, N., 2018. Late Miocene climate cooling and intensification of southeast Asian winter monsoon. Nature communications, 9(1), 1-13.

Miller., K.G., Baluyot, R., Wright, J.D., Kopp, R.E., Browning, J.V., 2017. Closing early Miocene astronomical gap with Southern Ocean 13C records:implications for sea level change. Paleoceanography, 32(6),600-621.

Ogg, J.G., Ogg, G., Gradsteins, F. M.A., 2016. Concise Geologic Time Scale: 2016. Elsevier, p. 234.

Perea, D., Martínez, S., 2004. Estratigrafíadel Mioceno–Pleistoceno en el litoral sur-oeste de Uruguay. Cuencas sedimentarias de Uruguay, Cenozoico (Veroslavsky, G., Ubilla, M. & Martínez, S., Eds.). Ediciones DIRAC, Facultad de Ciencias, Montevideo, 105-124.

Perea, D., Gutiérrez, G.D.M., Lorenzo, N., Martínez, S., Piñeiro, G., Lecuona, G.R., Rinderknecht, A., Rojas, A., Ubilla, M., Soto, M., Veroslavsky, G., Verde, M., 2011. Fósiles de Uruguay. DIRAC.

Zachos j., Pagani, M., Sloan, L., Thomas, E., Billups, K., 2001. Trends, rhythms, and aberrations in global climate 65 Ma to present. Science, 292(5517), 686-693.